Food Chemistry 337 (2021) 127978

Contents lists available at ScienceDirect

Food Chemistry

journal homepage: www.elsevier.com/locate/foodchem

Electrochemical analysis of specific catalase activity during development of *Aspergillus flavus* and its correlation with aflatoxin B1 production

Yanjing Yun[a,b], Zhisong Lu[a,b,*], Jing Yang[a,b], Taotao Liang[a,b], Gang Xiao[a,b], Yan Qiao[a,b,*], Yang Liu[c,*]

[a] Key Laboratory of Luminescence Analysis and Molecular Sensing (Southwest University), Ministry of Education, School of Materials & Energy, Southwest University, No. 1 Tiansheng Road, Chongqing 400715, PR China
[b] Institute for Clean Energy & Advanced Materials, School of Materials & Energy, Southwest University, No.1 Tiansheng Road, Chongqing 400715, PR China
[c] School of Food Science and Engineering, Foshan University, Foshan 528231, Guangdong, PR China

ARTICLE INFO

Keywords:
Catalase
Aflatoxin B_1
Electrochemical method
Biosensor
Aspergillus flavus

ABSTRACT

Aflatoxin B_1 (AFB_1) contamination causes huge economic losses. To explore the correlation between catalase (CAT) and AFB_1 production during fungal development, we fabricated an electrochemical CAT-activity sensor by measuring residual H_2O_2 after enzymatic degradation. The sensor made by palladium nanoparticles/carbonized bacterial cellulose nanocomposites exhibits a linear range over 0.5–3.5 U/mL and a detection limit of 0.434 U/mL. Both dry weight and CAT activity of mycelia continuously increase. But, the latter shows a greater increase than the former after three days. Specific CAT activity in crude enzyme extract of *A. flavus* was quantified. It maintains at ~25.00 U/mg for 3 days and enhances to 28.91 and 45.30 U/mg, respectively, on days 4 and 5. AFB_1 production follows the same trend. On days 4 and 5, AFB_1 concentration reaches 201.35 and 767.9 ng/mL, respectively. The positive correlation between specific CAT activity and AFB_1 production suggests that CAT is involved in AFB_1 biosynthesis.

1. Introduction

Mycotoxins, a class of highly toxic secondary metabolites produced by certain types of fungi, are widespread contaminants in foods and feeds, posing a threat to human and animal health (Begum & Samajpati, 2000; Sweeney & Dobson, 1999). As a mycotoxin, aflatoxin B1 (AFB1) is considered the most toxic, inducing acute necrosis, cirrhosis and hepatocellular carcinoma in humans (Castegnaro & Mcgregor, 1998; Rawal, Kim, & Coulombe, 2010; Shen, Shi, Lee, & Ong, 1994), and is classified as group I carcinogen (human carcinogen) by International Agency for Research on Cancer (IARC). Generally, AFB_1 is produced by *Aspergillus flavus* and *A. parasiticus*. It was found in various crop plants of peanuts, cotton-seed, corn, wheat, and other grains (Hussain, Khan, Khan, Javed, Saleemi, Mahmood, & Asi, 2010; Jaimez et al., 2000). Once the crops are contaminated, it is difficult to remove AFB_1, resulting in huge waste and economic losses (Maier et al., 2010). Therefore, significant efforts have been made to prevent AFB_1-contamination during production, harvesting, storage, and processing. Among these, storage is the most crucialstage for prevention, because of its relatively long period. Currently, a variety of parameters, such as temperature, gas composition, and microbial activity, are monitored to predict AFB_1 production (Abramson, Hulasare, White, Jayas, & Marquardt, 1999; Maier et al., 2010). These parameters can reflect the growth of mycotoxin-producing fungi. Hitherto, they are not correlated directly to AFB_1 production due to the complex microbial communities in grains and distinct capabilities of fungal strains on mycotoxin production.

During oxygen metabolism, various types of reactive oxygen species (ROS), such as superoxide ($O_2^{\cdot -}$), hydroxyl ion ($\cdot OH^-$), hydroxyl radical ($\cdot OH$), and hydrogen peroxide (H_2O_2), are continuously generated in microbes (Reverberi et al., 2012; Roze et al., 2015). They function as signal molecules to regulate cellular physiological processes (Aguirre, Ríos-Momberg, Hewitt, & Hansberg, 2005), but are also a prerequisite for AFB_1 generation (Jayashree & Subramanyam, 2000). The enhancement and repression of oxidative stress could influence the production of AFB_1 in *A. flavus* (Jayashree, Praveen Rao, & Subramanyam, 2000; Mahoney & Molyneux, 2004; Reverberi, Zjalic, Ricelli, Fabbri, & Fanelli, 2006). In our recent works, the role of ROS in AFB_1 biosynthesis has also been proven by measuring ROS secretion from *A. flavus* (Li, Li, Lu, Liu, & Li, 2015; Zhao, Wang, Xu, & Lu, 2017). However, it is still of

* Corresponding authors at: Key Laboratory of Luminescence Analysis and Molecular Sensing (Southwest University), Ministry of Education, School of Materials & Energy, Southwest University, No.1 Tiansheng Road, Chongqing 400715, PR China.
E-mail addresses: zslu@swu.edu.cn (Z. Lu), yanqiao@swu.edu.cn (Y. Qiao), liuyangg@hotmail.com (Y. Liu).

https://doi.org/10.1016/j.foodchem.2020.127978
Received 6 September 2019; Received in revised form 23 August 2020; Accepted 30 August 2020
Available online 05 September 2020
0308-8146/ © 2020 Elsevier Ltd. All rights reserved.

great challenge to monitor ROS because of their very short half-lifes. Catalase (CAT) is one of the critical enzymes in the biological defense system, which could promote the decomposition of H_2O_2 into molecular oxygen and water (Guan & Scandalios, 1995). Usually, microorganisms lived in an oxygenated environment could produce CAT to protect them from the toxic by-products of oxygen metabolism. As a vital enzyme regulating the intracellular ROS level, CAT could be possibly involved in the AFB_1 generation in *A. flavus*. Recent work has been made to investigate the relationship between CAT activity and AFB_1 amount by mimicking corn storage conditions (Zhang, Zhai, Zhang, & Cai, 2017), in which the suspension of microorganisms was directly used for monitoring CAT activity without a cell disruption procedure. Typically, the CAT catalytic activity of intact bacteria or fungi was measured to quantify the amount of CAT-positive microorganisms in a system (Hansberg, Salas-Lizana, & Dominguez, 2012; Reverberi, Ricelli, Zjalic, Fabbri, & Fanelli, 2010; Zhang et al., 2014) and cannot be utilized to reflect the total activity of intracellular CAT enzymes. Therefore, the findings may be affected by complex fungal communities, and the biomass increased during the corn storage process. The intracellular CAT activity should be monitored along with AFB_1 production throughout the fungal development to reveal the possible correlation between CAT and AFB_1.

UV–visible and colorimetric methods are conventionally utilized to measure CAT activity in the crude extract of different cells. However, their practical applications suffer from poor sensitivity. The rapid enhancement of CAT activity during the fungal growth cannot be easily detected with the conventional approaches. Thus, it is highly desirable to develop a novel method with good sensitivity for accurate detection of CAT activity in fungi. Electrochemical methods have been widely used to detect a variety of biomarkers in the past decades due to their high sensitivity and quick analysis speed (Chen, Cai, Ren, Wen, & Zhao, 2012; Feng, Wang, & Chen, 2009; Henzler & Steudle, 2000; Karyakin, 2001; Liu et al., 2012; Wang & Wang, 2004). The electrochemical H_2O_2 sensor has already been utilized to evaluate the amount of CAT-positive bacteria (Majumdar, Chakraborty, & Raychaudhuri, 2013). So far, it has not been employed to quantitatively measure intracellular CAT activity in fungi. Therefore, an electrochemical sensor may meet the requirements of CAT activity measurement throughout *A. flavus* development, further helping to reveal the correlation between CAT and AFB_1 production.

In the present work, we have fabricated an electrochemical H_2O_2 sensor with palladium nanoparticles (PdNPs)/carbonized bacterial cellulose (CBC) nanocomposites as the catalytic materials for competitive measurement of CAT activity in the crude enzyme extract of *A. flavus*. The PdNPs/CBC nanocomposites were characterized by field emission scanning electron microscopy (FESEM), transmission electron microscopy (TEM), and X-ray diffraction (XRD). The H_2O_2 sensing performance was examined with cyclic voltammetry (CV) and amperometric technique. The CAT standard solution or crude enzyme extract was pre-mixed with H_2O_2 to catalyze their decomposition. The remaining H_2O_2 in the mixture was measured with the as-prepared electrochemical sensor to quantitatively reflect CAT activity. The development of *A. flavus* was monitored by weighing dry mycelial pellets. The intracellular CAT activity and AFB_1 production at different developmental stages were evaluated with the electrochemical CAT sensor and high-performance liquid chromatography (HPLC) technique, respectively, to investigate the correlation between CAT and AFB_1. *A. flavus* was selected as the model fungus in the present study since it is the main AFB_1 producing fungal species in agricultural commodities (Lahouar, Crespo-Sempere, Marín, Saïd, & Sanchis, 2015; Xing, Liu, Chang, & Tai, 2020).

2. Experimental

2.1. Chemicals

Hydrogen peroxide (AR, 30%), ascorbic acid (AA), sodium borohydride, sucrose and $PdCl_2$ were purchased from Aladdin (Shanghai, P. R. China). CAT, uric acid (UA), potassium superoxide (KO_2), Nafion perfluorinated resin, and hexadecyl trimethyl ammonium bromide (CTAB) were bought from Sigma–Aldrich (Saint Louis, MO, USA). Bacterial cellulose nanofibers were obtained from Foshan Fibre-Bao nonwoven fabric products Co. Ltd. (Guangdong, P. R. China). Soybean peptone and yeast extract were obtained from Qingdao Hope Biotechnology Co. Ltd. (Qingdao, P. R. China). Other chemicals were of analytical grade and used without further purification. *A. flavus* GZ-6 was a gift from Institute of Agro-Products Processing Science and Technology, Chinese Academy of Agricultural Sciences, Beijing, P. R. China. Deionized (DI) water with the resistance over 18 MΩ·cm was generated with a Millipore water purification system.

2.2. Synthesis of PdNPs-CBC nanocomposite

Commercially available bacterial cellulose nanofibers were carbonized with a two-step approach in a high-temperature furnace under nitrogen atmosphere. Initially, the temperature was heated to 500 °C at a heating rate of 2 °C/min with the soak time of 1 h. Then, it was further enhanced to 900 °C at a rate of 5 °C/min, maintaining for another 2 h. After the furnace cooled to room temperature, the final products of carbonized bacterial cellulose (CBC) were collected and stored at ambient conditions for the following modifications.

The synthesis of PdNPs-CBC nanocomposite was conducted in a 50 mL round-bottom flask. Briefly, 66 mg CBC was suspended in 10 mL of 37.5 mM CTAB, stirring at 95 °C constantly for 20 min. 0.5 mL of 30 mM $PdCl_2$ solution was added into the mixture, stirring at 95 °C for another 30 min. Then, 80 μL of 0.3 M ascorbic acid was introduced into the above system at 95 °C to reduce Pd ions. Finally, the products were washed with pure water under centrifugation (10,000 rpm for 20 min) for several times, followed by freeze-drying.

2.3. Material characterization

FESEM (JSM-7800F, Joel, Japan) and TEM (JEM-2100, Joel, Japan) were carried out to characterize morphologies of CBC and PdNPs/CBC nanocomposites. During the measurements, materials were suspended in an ethanol solution and directly dropped on aluminum foils or TEM grids to prepare samples for SEM and TEM, respectively. XRD pattern of the PdNPs-CBC composites was obtained using a diffractometer (MAXima-X 7000, Japan) with Cu Kα source operated at 40 kV and 30 mA in the 2θ range of 10–90°.

2.4. Preparation of nanocomposite-modified electrode

Firstly, 2 mg PdNPs/CBC nanocomposites were ultrasonically dispersed in 1 mL DI water with 25 μL Nafion solution. Then, 6 μL of above suspension was cast on a glassy carbon electrode (GCE) surface, drying at room temperature to form a uniform thin film. Prior to the nanocomposite immobilization, the GCE surface was polished with alumina powder (Particle size: 0.5 and 0.05 μm) and thoroughly rinsed with DI water and ethanol.

2.5. Preparation of crude enzyme extracts from A. flavus

A. flavus was inoculated in 50 mL yeast extract with supplements medium (450 g/L sucrose, 60 g/L yeast extract, and 30 g/L soybean peptone in deionized water), culturing at 37 °C under 200 rpm shaking for 5 days. The mycelia pellets were sampled every 12 h. After filtration and repeated washing, the mycelia were suspended in 20 mL PBS

(0.1 mol/L, pH = 7.4). An ultrasonic cell disruptor (200 W) was used to break the *A. flavus* mycelia for 4 min, followed by centrifugation at 4000 rpm for 20 min. The supernatant was collected as the crude enzyme extract, storing at 4 °C for the following assays. During the culture process, weight of the mycelia pellets was also measured after drying at 80 °C for several hours to evaluate the growth of *A. flavus*.

2.6. Electrochemical measurements

Electrochemical experiments were performed by a CHI 660B electrochemical workstation (CH Instruments, Shanghai, China) with a conventional three-electrode system. A catalyst-immobilized GCE, a saturated Ag/AgCl electrode and a platinum wire were used as working, reference and counter electrodes, respectively. The supporting electrolyte was 0.1 M phosphate buffer solution (PBS) at pH 7.4. Prior to measurements, the solution was deoxygenated with nitrogen gas for 30 min. All electrochemical experiments were conducted at room temperature (25 ± 1 °C).

As to CAT activity analysis, different amount of pure CAT or crude enzyme extract was initially mixed with H_2O_2, incubating at room temperature for 2 min. Then, the mixture was added into PBS under stirring to measure the electrochemical response to H_2O_2. Since CAT catalyzes H_2O_2 decomposition, the measured current could be used to represent CAT activity in the sample.

2.7. AFB_1 measurement

During the culture process, 10 mL culture medium was collected at an interval of 12 h. The medium was mixed with 30 mL chloroform for 20 min at room temperature. After resting for 5 min, the chloroform solution was filtered to remove impurity. The filtered solution was diluted with pure water and passed through an immunoaffinity column. The AFB_1 concentration was determined by high performance liquid chromatography (HPLC) coupled with a fluorescence detector (excitation wavelength of 360 nm; emission wavelength of 440 nm) using C18 column.

3. Results and discussion

3.1. Characterization of PdNPs/CBC nanocomposites

Morphology of pristine CBC and PdNPs/CBC nanocomposites was characterized by FESEM and TEM (Fig. 1). The CBC sample shows a lot of nanofibers and nanobelts, which are crosslinked with each other to form a three-dimensional '*network-like*' structure (Fig. 1a and c). After chemical deposition, a considerable amount of PdNPs are attached on nanofibers and nanobelts (Fig. 1b). A closer view of PdNPs/CBC nanocomposites in the high-magnification TEM image further exhibits that the PdNPs are well dispersed on the nanofibers surface with an average diameter of ~20 nm (Fig. 1d). XRD pattern was collected to further verify the crystalline structure of PdNPs/CBC nanocomposites (Fig. S1 in ESI). A broad diffraction peak appears at 20–30°, which can be indexed to the amorphous carbon. The weak peaks at 40.1° and 46.7° can be assigned to the diffraction of Pd [1 1 1] and [2 0 0] planes, respectively, suggesting that the as-prepared PdNPs have a typical face-centered-cubic structure. The results indicate that PdNPs with good crystalline structures are successfully anchored on CBC networks, and the particle size falls in the range of PdNPs with high catalytic activity.

3.2. Electrocatalytic behavior of PdNPs/CBC nanocomposites

The PdNPs/CBC nanocomposites were immobilized on GCE to fabricate the electrochemical H_2O_2 sensor. As illustrated by CV curves collected in $K_3[Fe(CN)_6]$ (Fig. S2a in ESI), the modification of PdNPs/CBC nanocomposites could significantly enhance the redox peak currents, which may be attributed to the 3D nanostructures with excellent conductivity. The smallest semicircle in the Nyquist plots (Fig. S2b in ESI) also indicates the fast charge transfer rate of the modified electrode. Electrocatalytic activity of the PdNPs/CBC nanocomposites toward H_2O_2 reduction was investigated by CV in N_2-saturated 0.1 M PBS. As shown in Fig. 2a, there is no peak in the absence of H_2O_2. However, in the presence of 5 mM H_2O_2, a remarkably catalytic peak could be observed at around −0.27 V, corresponding to H_2O_2 reduction on the PdNPs/CBC-modified GCE. The reaction could be expressed with the following equations (Liu et al., 2012):

$$H_2O_2 + e^- \rightarrow OH_{ad} + OH^- \quad (1)$$

$$OH_{ad} + e^- \rightarrow OH^- \quad (2)$$

$$2OH^- + 2H^+ \rightarrow 2H_2O \quad (3)$$

To understand the catalytic process, CVs of the modified electrode was scanned at the rates ranging from 20 to 140 mV/s (Fig. 2b). The cathodic peak current is increased with directly proportional to the scan rate in the whole range, suggesting that the electrocatalytic reduction of H_2O_2 on the modified electrode is a surface-confined process. The above data show that the PdNPs/CBC nanocomposites have good electrocatalytic activity toward H_2O_2 reduction. The PdNPs/CBC-modified GCE could be used as an electrochemical sensor for sensitive and selective detection of H_2O_2.

3.3. Electrochemical responses to H_2O_2

In order to further evaluate H_2O_2 sensing performance, the amperometric response of the modified electrode to H_2O_2 was recorded at an applied potential of −0.25 V in 0.1 M PBS (pH 7.4) under slow stirring (Fig. 3a). The potential was selected based on the optimization data as shown in Fig. S3 of ESI. With the successive addition of H_2O_2, the reduction current exhibits a stepped enhancement (Fig. 3a) until the H_2O_2 concentration reaches to 39.29 mM. A significant increase of the reduction current could be easily differentiated from the current–time trace upon the injection of 0.1 mM H_2O_2 (Inset of Fig. 3a). There is a linear relationship between reduction current and H_2O_2 concentration over the range of 0.1–39.29 mM (Fig. 3b) with the detection limit of 73.70 μM (S/N = 3) and sensitivity of 115.23 μA/(mM·cm^2). In comparison to reported electrochemical H_2O_2 sensors (Table S1 in the supporting information), the as-prepared sensor exhibits a wider linear range and a comparable detection limit, which are of great significance for sensitive detection of CAT activity in the present study. To investigate the anti-interference capability, 1 mM of H_2O_2, uric acid (UA), ascorbic acid (AA), and $O_2^{\cdot -}$ were successively added into 0.1 M PBS (pH 7.4). In contrast to the remarkable responses to H_2O_2, no response occurs to any of the interferences (Fig. 3c), showing the excellent selectivity of the PdNPs/CBC-modified electrode. The H_2O_2 sensing performance could fulfill the requirements of CAT activity measurement in the following experiments.

3.4. Electrochemical method for CAT activity monitoring

Since CAT could catalyze H_2O_2 decomposition, the addition of CAT in a mixture containing a certain amount of H_2O_2 could result in the decrease of H_2O_2 concentration. Therefore, the as-prepared electrochemical sensor could quantitatively evaluate CAT activity in the system by monitoring the remaining H_2O_2. A series of diluted CAT standard solutions were pre-mixed with 10 mM H_2O_2, incubating at room temperature for 2 min to enable the catalytic reactions. Then, amperometric tests were conducted to monitor the current changes upon the addition of above mixtures (Fig. 4a). The current change data could be used to represent CAT activity in the system. As rising of CAT activity, the current change gradually decreases, agreeing well with the detection mechanism. The current change is linearly correlated to CAT activity in the range of 0.5–3.5 U/mL (R^2 = 0.98) with a slope of

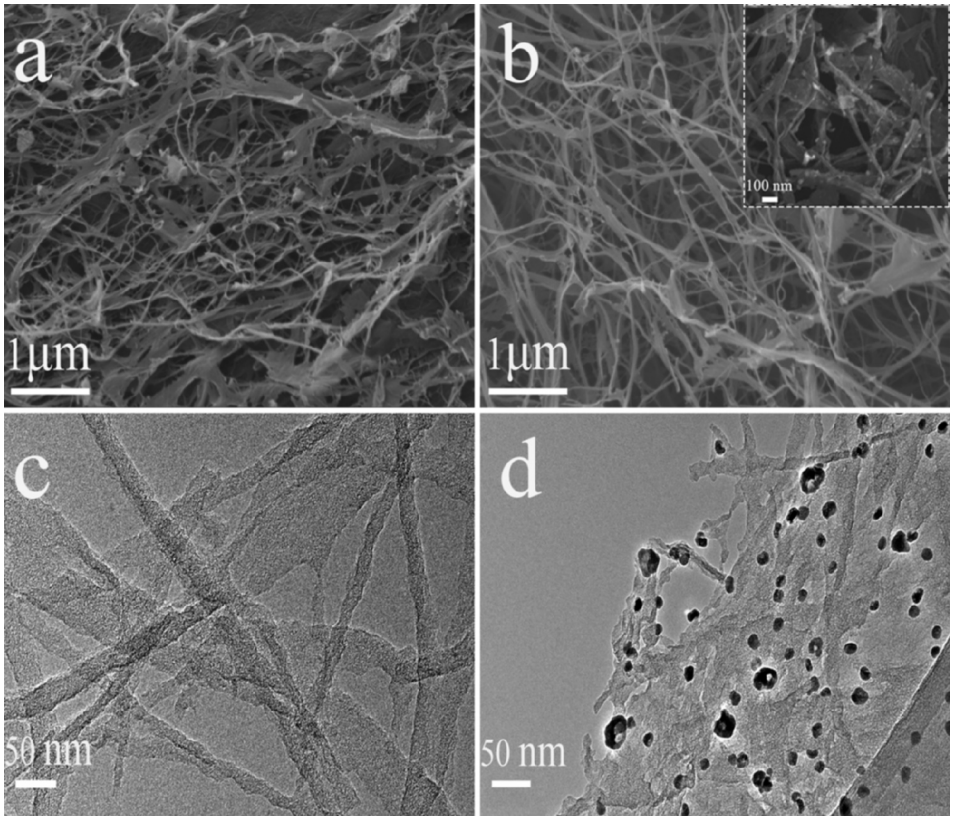

Fig. 1. Morphologies of CBC (a, c) and PdNPs/CBC nanocomposites (b, d). (a) and (b) FESEM images; (c) and (b) TEM images.

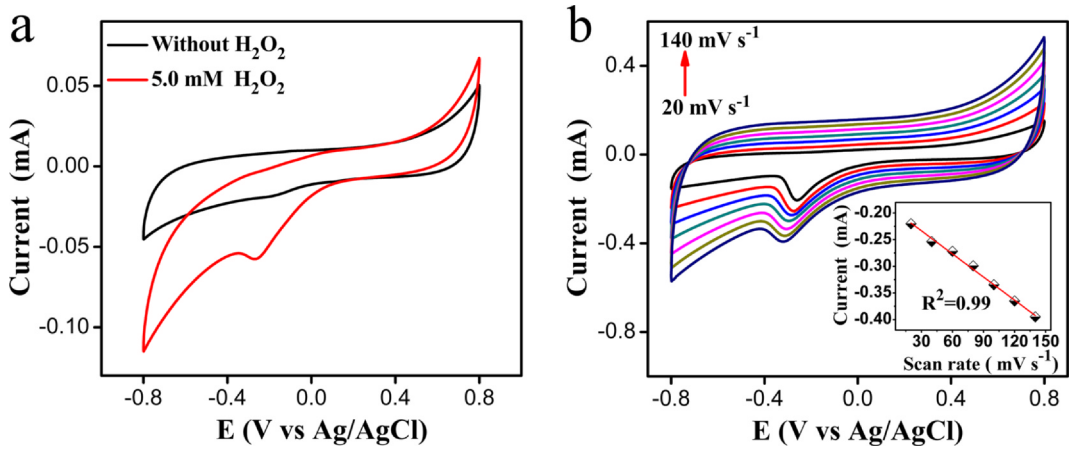

Fig. 2. (a) Cyclic voltammetry behavior of PdNPs-CBC nanocomposites-modified GCE in N_2-saturated 0.1 M PBS at pH 7.4 in the absence (black curve) and presence (red curve) of 5.0 mM H_2O_2 at the scan rate of 50 mV/s, respectively; (b) CV of PdNPs/CBC nanocomposites-modified GCE in N_2-saturated 0.1 M PBS containing 5.0 mM H_2O_2 at pH 7.4 at different scan rates. Inset: Linear plots of peak current *vs*. scan rate. (For interpretation of the references to colour in this figure legend, the reader is referred to the web version of this article.)

−5.8688 (Fig. 4b). In order to verify reliability of the proposed method for the CAT activity detection, the traditional approach based on UV spectrophotometry was also carried out for comparison (Fig. S4 in ESI), demonstrating that the electrochemical method possesses higher sensitivity and a wider detection range. Moreover, the detection limit is calculated to be 0.434 U/mL, which is lower than those of Catalase Assay Kits available in the market (0.5 U/mL for K-CATAL, Megazyme Ltd.; 1 U/mL for S0051, Beyotime Ltd.). As previously reported, the average catalase activity in raw milk, human blood plasma, and fresh wheatgrass juice are 1.95, 86, and 213.28 U/mL, respectively (Hirvi & Griffiths, 1998; Simic et al., 2006). Thus, the as-prepared electrochemical CAT sensor has great potentials in practical applications.

3.5. Measurements of CAT activity in crude enzyme extract from *A. flavus*

In the present study, *A. flavus* was cultured in liquid medium for 5 days, during which growth of *A. flavus* was monitored by examining dry weight of the mycelia (Fig. 5a). From the 1st day to 3rd day, the amount of biomass in culture medium sharply increases, indicating the fast growth of *A. flavus*. After 3 days of culture, the dry weight still gradually rises, but the rate slows down. The trend matches well with the development of *A. flavus* from spores to mycelium balls. During the development process, CAT activity in the crude enzyme extract were also measured with the constructed electrochemical sensor. As the elongation of culture duration, the current change gradually decreases

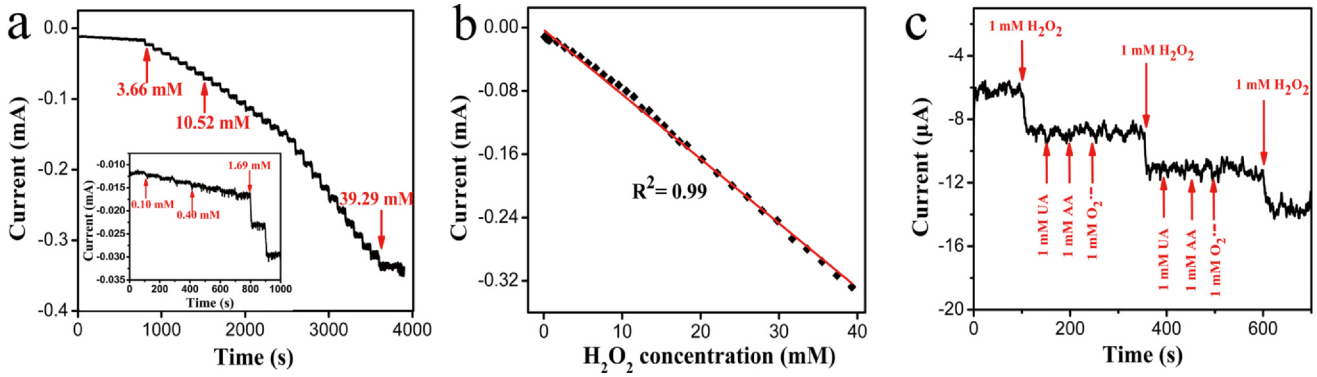

Fig. 3. (a) Amperometric responses of the PdNPs/CBC-modified electrode to successive additions of different concentrations of H_2O_2 at −0.25 V in 0.1 M PBS; (b) Plots of current density against H_2O_2 concentration; (c) Amperometric responses of the PdNPs/CBC-modified electrode to different analytes at −0.25 V in 0.1 M PBS.

from 28.46 ± 0.04 (1st day) to 16.47 ± 0.10 μA (5th day), suggesting the enhancement of CAT activity in the crude extract during fungal development (Fig. 5b). After quantitative calculation based on the calibration curve (Fig. 4b), total CAT activity in the culture system were plotted against duration (Fig. 5c). It can be seen that there is a positive correlation between CAT activity and culture time. The decomposition of H_2O_2 has been used to quantitatively detect CAT-positive bacteria (Majumdar et al., 2013). Surprisingly, it is found that the growing trend of *A. flavus* is significantly different from that of total CAT activity measured from the crude enzyme extracts, in particular after 4 days (Fig. 5a and c). The data may suggest abnormal intracellular ROS metabolism at the late developmental stage of *A. flavus*.

3.6. Correlation between specific CAT activity and AFB_1 production

Since the remarkable increase of biomass may contribute to total enzyme activity during the early developmental stage, specific CAT activity was calculated by dividing total CAT activity with the dry weight to investigate the dynamic change of CAT activity per unit mass of mycelium. The specific CAT activity could be calculated with the following equation:

$$Specific\ CAT\ activity = \frac{Total\ CAT\ activity}{Dry\ weight}$$

As shown in Fig. 6 (black curve), during the first 3 days, there is no obvious alteration on the specific CAT activity, strongly proving the contribution of biomass on the total enzyme activity. At this stage, the intracellular ROS may be maintained at a normal level that could promote the rapid development of *A. flavus*. The balance between oxidative stress and anti-oxidative system is very stable. However, a sharp increase in the specific CAT activity appears on days 4 and 5, which may be the response of cellular anti-oxidative system to the ROS accumulation. After 3 days, the nutrition in culture medium is insufficient to support fast fungal growth. At this stage, ROS starts to accumulate, and the anti-oxidative enzyme is expressed to protect cells from the oxidative damage.

The amount of AFB_1 in culture medium was analyzed with HPLC after culturing for 1–5 days. The AFB_1 concentration was plotted against culture duration to investigate the production of AFB_1 from each mycelium (Fig. 6, red curve and Table S2 in ESI). During the first 3 days, AFB_1 production maintains at a relatively low level. However, from day 3 to day 5, the AFB_1 amount exhibits an explosive growth. The accumulated AFB_1 concentration are 201.35 ± 10.96 and 767.9 ± 35.64 ng/mL on days 4 and 5, respectively. As shown in Fig. 5a, A. *flavus* grows rapidly during the first 3 days. The primary metabolites are consumed by fungal cells to promote their development and growth, resulting in the low production of secondary metabolites including AFB_1. At the late developmental stage, the growth of fungi slows down due to the lack of nutritional factors. Thus, secondary metabolism occurs and *A. flavus* undergoes a switch from biomass

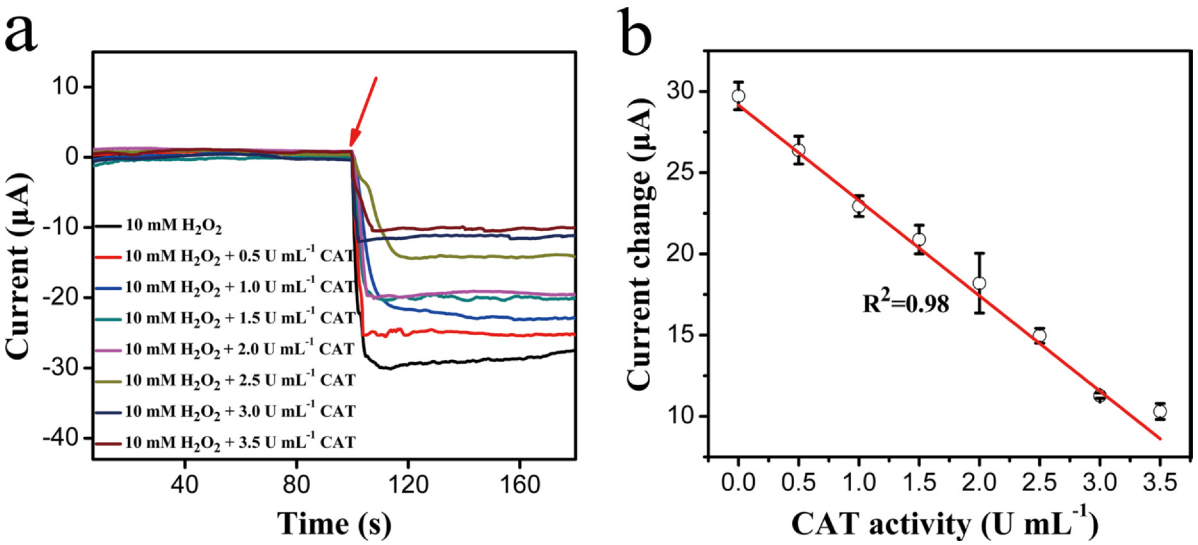

Fig. 4. (a) Amperometric responses of the PdNPs/CBC-modified electrode to the addition of mixtures containing 10 mM H_2O_2 and different amounts of CAT; The red arrow indicates the time for the addition of the mixtures; (b) Plots of response current against CAT activity. (For interpretation of the references to colour in this figure legend, the reader is referred to the web version of this article.)

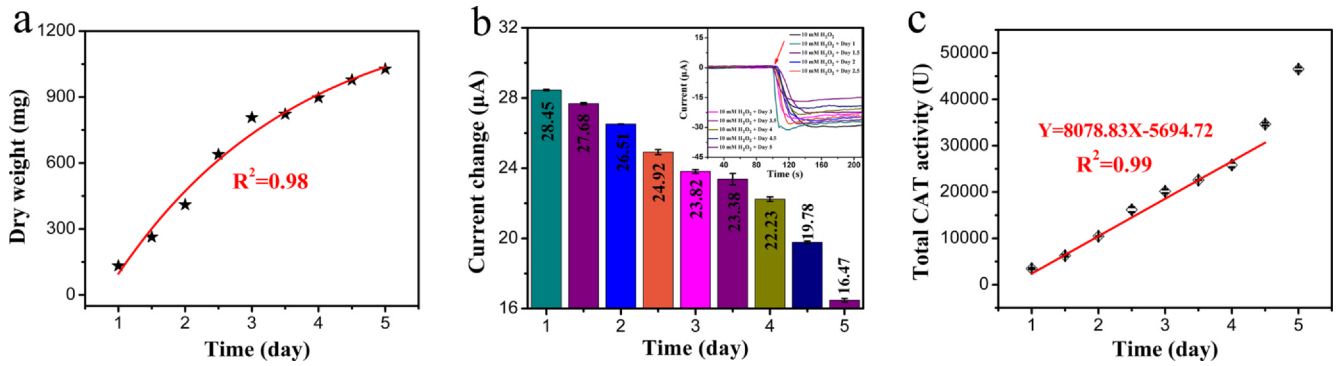

Fig. 5. (a) Change of dry weight of *A. flavus* during the culture period; (b) Amperometric responses of the PdNPs/CBC-modified electrode to the addition of mixtures containing 10 mM H_2O_2 and crude enzyme extracts on 1–5 days; (c) Plots of total CAT activity in the crude extract against culturing time.

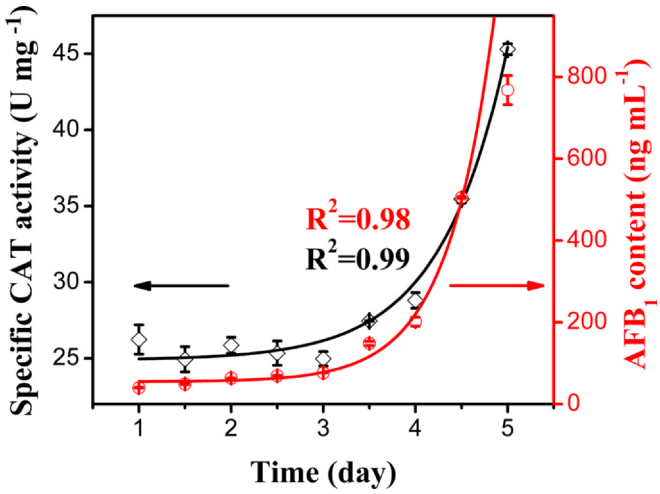

Fig. 6. Change of specific CAT activity (black curve) and AFB_1 production (red curve) in *A. flavus* during the culture process. (For interpretation of the references to colour in this figure legend, the reader is referred to the web version of this article.)

production to the production of secondary metabolites. Interestingly, during the development of *A. flavus,* AFB_1 production and specific CAT activity demonstrate the same alteration trend, which may suggest the potential correlation between CAT activity and AFB_1 production. Our statistical analysis also shows that there is a positive correlation between specific CAT activity and AFB_1 production in the *A. flavus* ($R^2 = 0.98$, $p < 0.05$). ROS have been considered as the prerequisite for AFB_1 generation (Jayashree & Subramanyam, 2000; Li et al., 2015; Zhao et al., 2017). The AFB_1 production in *A. flavus* could also be affected by the intracellular oxidative stress (Jayashree et al., 2000; Mahoney & Molyneux, 2004; Reverberi et al., 2006). Under the stimulation of oleic acid, both CAT activity and gene expression of aflatoxin significantly increases in *Aspergillus* strains (Maggiohall, Wilson, & Keller, 2005). Based on the literatures and experimental data, it could be speculated that both AFB_1 production and enhancement of specific CAT activity may be triggered by the formation of oxidative stress in *A. flavus.* Therefore, CAT activity per unit of biomass could be possibly applied in the practical applications as the indicator of AFB_1 production in the *A. flavus*-contaminated system.

4. Conclusions

In summary, a sensitive H_2O_2 electrochemical biosensor was fabricated with PdNPs/CBC nanocomposites as catalytic materials for analysis of CAT activity in the crude extract of mycelia during the culture process. The fabricated sensor could measure CAT activity over the range of 0.5–3.5 U/mL ($R^2 = 0.98$) with a detection limit of 0.434 U/mL. Both sensitivity and detection range are better than those of the conventional UV spectrophotometry-based method. The total CAT activity in the crude enzyme extract from the mycelia increases linearly as the elongation of culture duration. Considering the contribution of biomass, specific CAT activity is calculated by dividing total CAT activity with dry weight of mycelia. Results show that the specific CAT activity does not change during the first three days, but rapidly enhances on days 4 and 5. The AFB_1 production also demonstrates the same trend during the culture period. Based on the findings, it could be concluded that the specific CAT activity may be closely correlated with AFB_1 production in *A. flavus*. Specific CAT activity could be possibly used as a promising indicator for AFB_1 production in the food storage process.

CRediT authorship contribution statement

Yanjing Yun: Methodology, Software, Data curation, Writing - original draft, Investigation, Writing - review & editing. **Zhisong Lu:** Conceptualization, Supervision, Writing - review & editing. **Jing Yang:** Methodology, Supervision, Validation, Writing - review & editing. **Taotao Liang:** Methodology, Software, Investigation. **Gang Xiao:** Methodology, Software, Data curation. **Yan Qiao:** Methodology, Software, Supervision, Writing - review & editing. **Yang Liu:** Conceptualization, Methodology, Supervision, Writing - review & editing.

Declaration of Competing Interest

The authors declare that they have no known competing financial interests or personal relationships that could have appeared to influence the work reported in this paper.

Acknowledgments

This work is financially supported by National Key R&D Program of China (2019YFC1604500), Fundamental Research Funds for the Central Universities (XDJK2019B002), Chongqing Natural Science Foundation (cstc2019jcyj-msxmX0314) and Chongqing Engineering Research Center for Micro-Nano Biomedical Materials and Devices.

Appendix A. Supplementary data

Supplementary data to this article can be found online at https://doi.org/10.1016/j.foodchem.2020.127978.

References

Abramson, D., Hulasare, R., White, N. D. G., Jayas, D. S., & Marquardt, R. R. (1999).

Mycotoxin formation in hulless barley during granary storage at 15 and 19% moisture content. *Journal of Stored Products Research, 35*(3), 297–305.
Aguirre, J., Ríos-Momberg, M., Hewitt, D., & Hansberg, W. (2005). Reactive oxygen species and development in microbial eukaryotes. *Trends in Microbiology, 13*(3), 111–118.
Begum, F., & Samajpati, N. (2000). Mycotoxin production on rice, pulses and oilseeds. *Naturwissenschaften, 87*(6), 275–277.
Castegnaro, M., & Mcgregor, D. (1998). Carcinogenic risk assessment of mycotoxins. *Revue De Medecine Veterinaire, 149*(6), 671–678.
Chen, W., Cai, S., Ren, Q. Q., Wen, W., & Zhao, Y. D. (2012). Recent advances in electrochemical sensing for hydrogen peroxide: A review. *Analyst, 137*(1), 49–58.
Feng, D., Wang, F., & Chen, Z. (2009). Electrochemical glucose sensor based on one-step construction of gold nanoparticle–chitosan composite film. *Sensors and Actuators B: Chemical, 138*(2), 539–544.
Guan, L. M., & Scandalios, J. G. (1995). Developmentally related responses of maize catalase genes to salicylic acid. *Proceedings of the National Academy of Sciences of the United States of America, 92*(13), 5930–5934.
Hansberg, W., Salas-Lizana, R., & Dominguez, L. (2012). Fungal catalases: Function, phylogenetic origin and structure. *Archives of Biochemistry and Biophysics, 525*(2), 170–180.
Henzler, T., & Steudle, E. (2000). Transport and metabolic degradation of hydrogen peroxide in Chara corallina: Model calculations and measurements with the pressure probe suggest transport of H_2O_2 across water channels. *Journal of Experimental Botany, 51*(353), 2053–2066.
Hirvi, Y., & Griffiths, M. W. (1998). Milk catalase activity as an indicator of thermization treatments used in the manufacture of cheddar cheese. *Journal of Dairy Science, 81*(2), 338–345.
Hussain, Z., Khan, M. Z., Khan, A., Javed, I., Saleemi, M. K., Mahmood, S., & Asi, M. R. (2010). Residues of aflatoxin B1 in broiler meat: Effect of age and dietary aflatoxin B1 levels. Food and Chemical Toxicology, 48(12), 3304-3307.
Jaimez, J., Fente, C. A., Vazquez, B. I., Franco, C. M., Cepeda, A., Mahuzier, G., & Prognon, P. (2000). Application of the assay of aflatoxins by liquid chromatography with fluorescence detection in food analysis. *Journal of Chromatography A, 882*(1–2), 1–10.
Jayashree, T., & Subramanyam, C. (2000). Oxidative stress as a prerequisite for aflatoxin production by Aspergillus parasiticus. *Free Radical Biology and Medicine, 29*(10), 981–985.
Jayashree, T., Praveen Rao, J., & Subramanyam, C. (2000). Regulation of aflatoxin production by Ca^{2+}/calmodulin-dependent protein phosphorylation and dephosphorylation. *FEMS Microbiology Letters, 183*(2), 215–219.
Karyakin, A. A. (2001). Prussian blue and its analogues: Electrochemistry and analytical applications. *Electroanalysis, 13*(10), 813–819.
Lahouar, A., Crespo-Sempere, A., Marín, S., Saïd, S., & Sanchis, V. (2015). Toxigenic molds in Tunisian and Egyptian sorghum for human consumption. *Journal of Stored Products Research, 63*, 57–62.
Li, J., Li, J., Lu, Z., Liu, Y., & Li, C. M. (2015). Transient transmembrane secretion of H_2O_2: A mechanism for the citral-caused inhibition of aflatoxin production from Aspergillus flavus. *Chemical Communications, 51*(98), 17424–17427.
Liu, R., Li, S., Yu, X., Zhang, G., Zhang, S., Yao, J., ... Zhi, L. (2012). Facile Synthesis of Au-nanoparticle/polyoxometalate/graphene tricomponent nanohybrids: An enzyme-free electrochemical biosensor for hydrogen peroxide. *Small, 8*(9), 1398–1406.
Maggiohall, L. A., Wilson, R. A., & Keller, N. P. (2005). Fundamental contribution of β-oxidation to polyketide mycotoxin production in planta. *Molecular Plant-microbe Interactions, 18*(8), 783–793.
Mahoney, N., & Molyneux, R. J. (2004). Phytochemical inhibition of aflatoxigenicity in Aspergillus flavus by constituents of walnut (Juglans regia). *Journal of Agricultural and Food Chemistry, 52*(7), 1882–1889.
Maier, D. E., Channaiah, L. H., Martinez-Kawas, A., Lawrence, J., Chaves, E., Coradi, P., & Fromme, G. (2010). Monitoring carbon dioxide concentration for early detection of spoilage in stored grain. *Julius-Kühn-Archiv, 425*, 512–516.
Majumdar, T., Chakraborty, R., & Raychaudhuri, U. (2013). Rapid electrochemical quantification of food borne pathogen staphylococcus aureus based on hydrogen peroxide degradation by catalase. *Journal of The Electrochemical Society, 160*(4), G75–G78.
Rawal, S., Kim, J. E., & Coulombe, R., Jr (2010). Aflatoxin B_1 in poultry: Toxicology, metabolism and prevention. *Research in Veterinary Science, 89*(3), 325–331.
Reverberi, M., Ricelli, A., Zjalic, S., Fabbri, A. A., & Fanelli, C. (2010). Natural functions of mycotoxins and control of their biosynthesis in fungi. *Applied Microbiology and Biotechnology, 87*(3), 899–911.
Reverberi, M., Punelli, M., Smith, C. A., Zjalic, S., Scarpari, M., Scala, V., ... Fabbri, C. (2012). How Peroxisomes affect aflatoxin biosynthesis in aspergillus flavus. *PLOS ONE, 7*(10), Article e48097.
Reverberi, M., Zjalic, S., Ricelli, A., Fabbri, A. A., & Fanelli, C. (2006). Oxidant/antioxidant balance in Aspergillus parasiticus affects aflatoxin biosynthesis. *Mycotoxin Research, 22*(1), 39–47.
Roze, L. V., Laivenieks, M., Hong, S. Y., Wee, J., Wong, S. S., Vanos, B., ... Linz, J. E. (2015). Aflatoxin biosynthesis is a novel source of reactive oxygen species—a potential redox signal to initiate resistance to oxidative stress? *Toxins, 7*(5), 1411–1430.
Simic, D. V., Mimic-Oka, J., Pljesa-Ercegovac, M., Savic-Radojevic, A., Opacic, M., Matic, D., ... Simic, T. (2006). Byproducts of oxidative protein damage and antioxidant enzyme activities in plasma of patients with different degrees of essential hypertension. *Journal of Human Hypertension, 20*(2), 149–155.
Shen, H. M., Shi, C. Y., Lee, H. P., & Ong, C. N. (1994). Aflatoxin B_1-induced lipid peroxidation in rat liver. *Toxicology and Applied Pharmacology, 127*(1), 145–150.
Sweeney, M. J., & Dobson, A. D. (1999). Molecular biology of mycotoxin biosynthesis. *FEMS Microbiology Letters, 175*(2), 149–163.
Wang, L., & Wang, E. (2004). A novel hydrogen peroxide sensor based on horseradish peroxidase immobilized on colloidal Au modified ITO electrode. *Electrochemistry Communications, 6*(2), 225–229.
Xing, F., Liu, Y., Chang, J., & Tai, B. (2020). Recent progress of the effect of environmental factors on Aspergillus flavus growth and aflatoxins production on foods. *Food Quality and Safety, 4*(1), 21–28.
Zhang, S. B., Zhai, H. C., Hu, Y. S., Wang, L., Yu, G. H., Huang, S. X., & Cai, J. P. (2014). A rapid detection method for microbial spoilage of agro-products based on catalase activity. *Food Control, 42*, 220–224.
Zhang, Y. L., Zhai, Zhang, H. C., & Cai, J. P. (2017). Early warning of AFB1 contamination in stored maize by monitoring catalase activity. *Food and Machinery, 33*(1), 110–113.
Zhao, J., Wang, L., Xu, D., & Lu, Z. (2017). Involvement of ROS in nanosilver-caused suppression of aflatoxin production from Aspergillus flavus. *RSC Advances, 7*(37), 23021–23026.